

## SENSOR PROPERTIES OF DUAL CORE OPTICAL FIBERS

© Wójcik J., Janoszczak B., Poturaj K., Klimek J., 2004

The series of the dual core optical fibers with the same dimensions of cores and numerical apertures but with different distance between cores was manufactured. To characterize these fibers their spectral attenuation, cut-off wavelength, coupling length, temperature sensitivity and pressure sensitivity were measured. The measurements of temperature sensitivity and pressure sensitivity for different polarizations of input light were done.

### 1. Introduction

During the last years, a new generation of optical fiber sensors using highly birefringent fibers, especially pressure and temperature sensors has been developed. The working principle on which they are based is the variation of the birefringence of optical fibers when they are submitted to different conditions of pressure and temperature [1].

Dual core fibers with circular shape of the cores were used for fiber couplers and switching purposes [2].

Polarization coupling spectra of dual elliptical core fibers were examined toward application in fiber polarization devices [3].

In this paper we present dual circular shape core optical fiber in which the working principle depends on the change of the coupling length when they are submitted to different conditions of pressure and temperature.

In our laboratory we elaborated technology of manufacturing dual core optical fibers and produced series of those fibers with the same dimensions of cores and numerical apertures but with different distance between cores.

To characterize manufactured fibers we measured their spectral attenuation, cut-off wavelength, coupling length, temperature sensitivity and pressure sensitivity. The measurements of temperature sensitivity and pressure sensitivity for different polarizations of input light were done.

For the optical measurements we adapted measurements methods used to characterization the low and high birefringent optical fibers.

### 2. Technology of the dual core optical fiber

Fig. 1 presents projected structure of the dual core optical fiber.

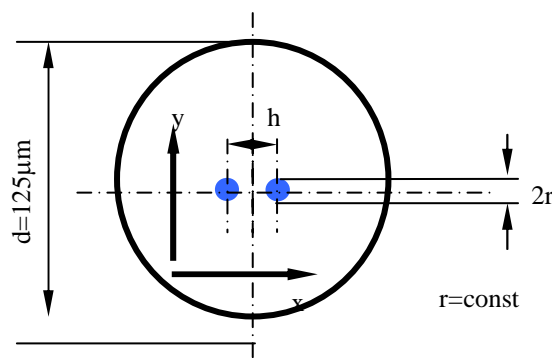


Fig. 1. Schema of the dual core optical fiber

The all optical fibers were manufactured with MCVD method from the same preform I with refractive index profile presented in fig. 2.

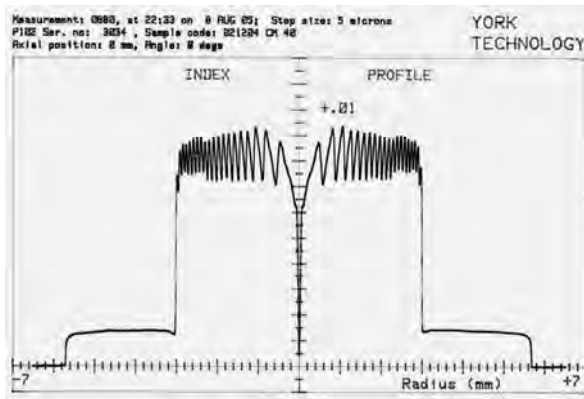


Fig. 2. Refractive index profile of the preform I

From this preform the small diameter rods were drawn and then from these rods the preforms II in the overcladding processes were manufactured. These preforms II was milled to “D” shape. Then the preform was obtained during the next overcladding process. Next the dual core optical fibers were manufactured from this preform in the drawing process. Fig. 3 presents the microscopic photos of drawn fibers.

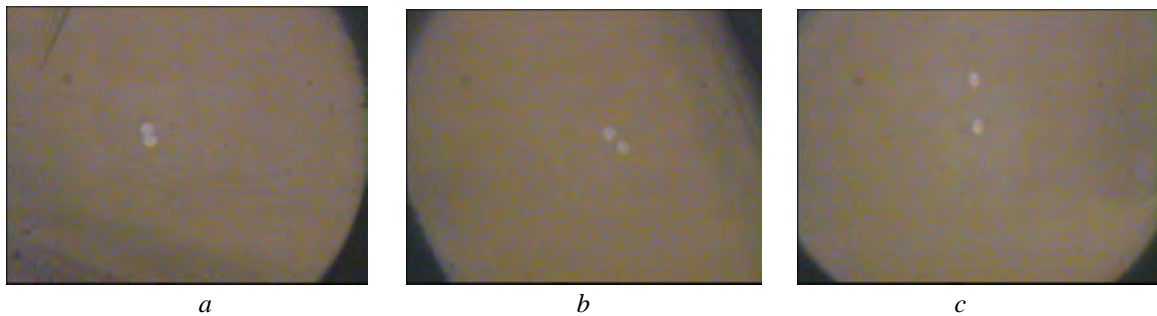


Fig. 3. The microscopic photos of drawn fibers:

$$2r = 3\mu\text{m}, h = 3,5\mu\text{m}, d = 125\mu\text{m};$$

$$2r = 3\mu\text{m}, h = 6\mu\text{m}, d = 125\mu\text{m};$$

$$2r = 3\mu\text{m}, h = 10\mu\text{m}, d = 125\mu\text{m}$$

### 3. Measurements

The some measurements were done to characterize the manufactured dual core optical fibers. The spectral attenuation was measured with cut-back method. The cutoff wavelength was measured with the loop attenuation method. The geometrical parameters were measured with the optical microscope with high resolution. The coupling length was measured with method analogous to measurement of the beat length for high birefringence optical fibers

Obtained results are presented in table 1.

Table 1

#### Results of measurement of some optical parameters of the dual core optical fibers

No	h [ $\mu\text{m}$ ]	h/r ratio	Cutoff wavelength $\lambda_c$ [ $\mu\text{m}$ ]	Coupling length [mm]
1.	3	2	1,05	-
2.	3,5	2,3	0,98	-
3.	6	4	0,79	-
4.	7	4,67	0,75	6,7
5.	10	6,67	0,69	25
6.	13	8,67	0,67	30

Fig. 4. presents spectral attenuation plot of the dual core optical fiber with  $h=6\mu\text{m}$  and  $2r=3\mu\text{m}$ .

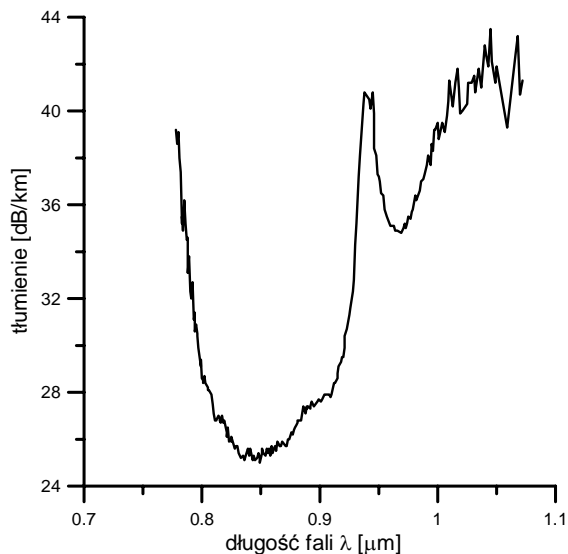


Fig. 4. The spectral attenuation of dual core optical fiber with  $h=6\mu\text{m}$  and  $2r=3\mu\text{m}$

The measurements of sensor properties e.g. pressure and temperature sensitivity of the dual core optical fibers were done with the set presented in fig. 5. The measurements of temperature and pressure sensitivity were done for different input light polarizations. The examined polarizations of output light were different too. Obtained results were interpreted in the following manner: When the temperature or pressure was changed, the brightness of the cores was changed too. The cycle: bright core – dark core – bright core, in our measurements means that the phase change about  $\pi$  radians

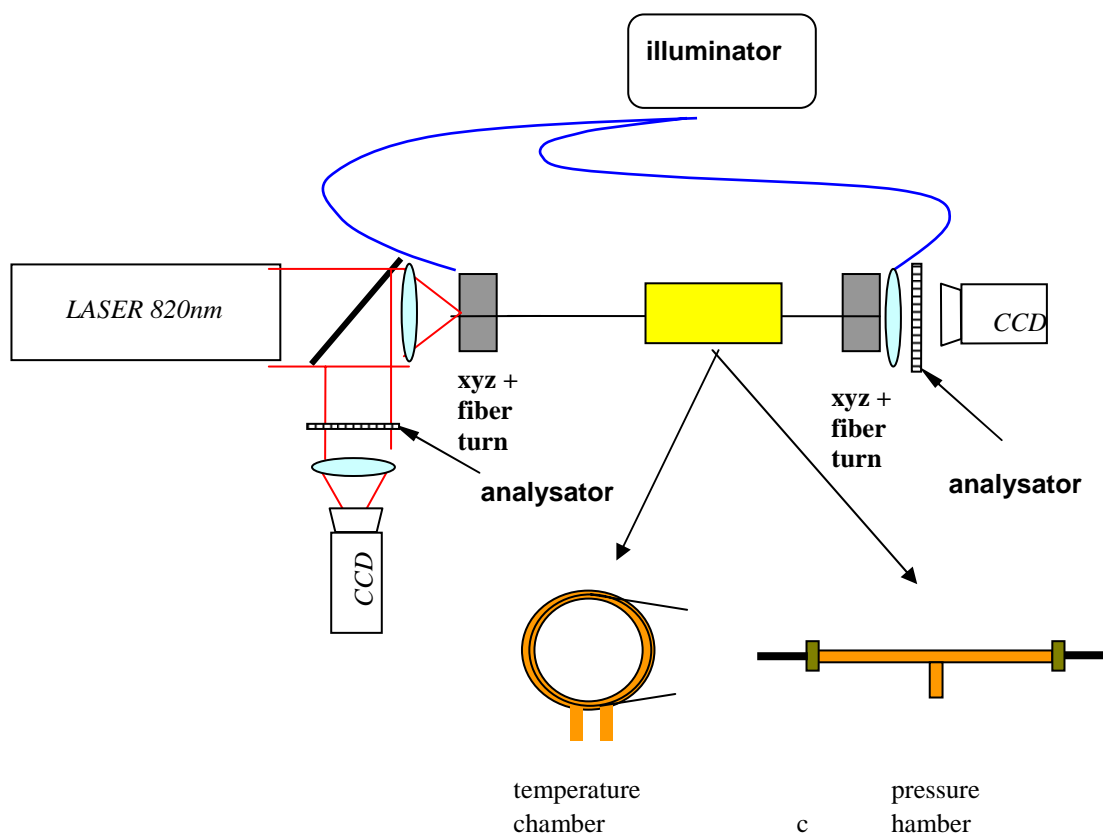
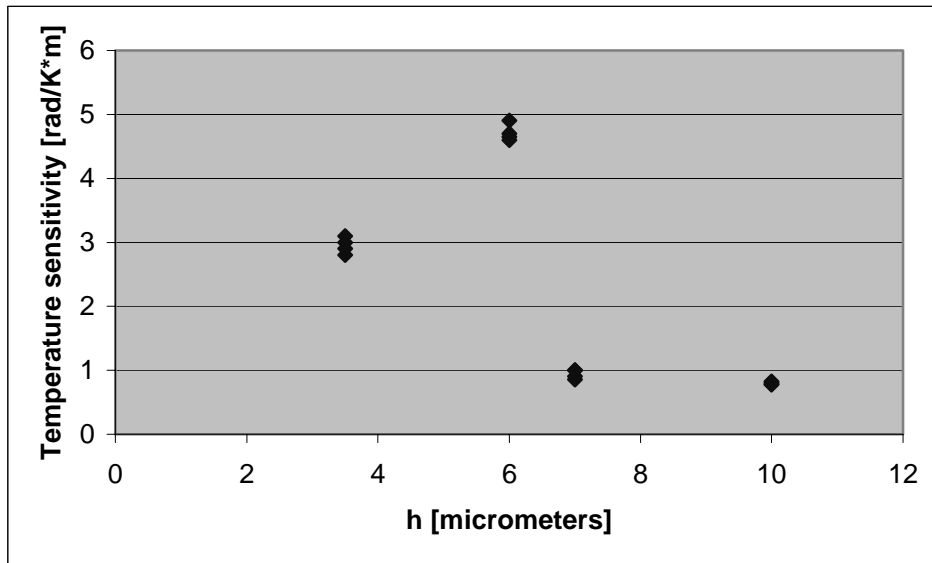


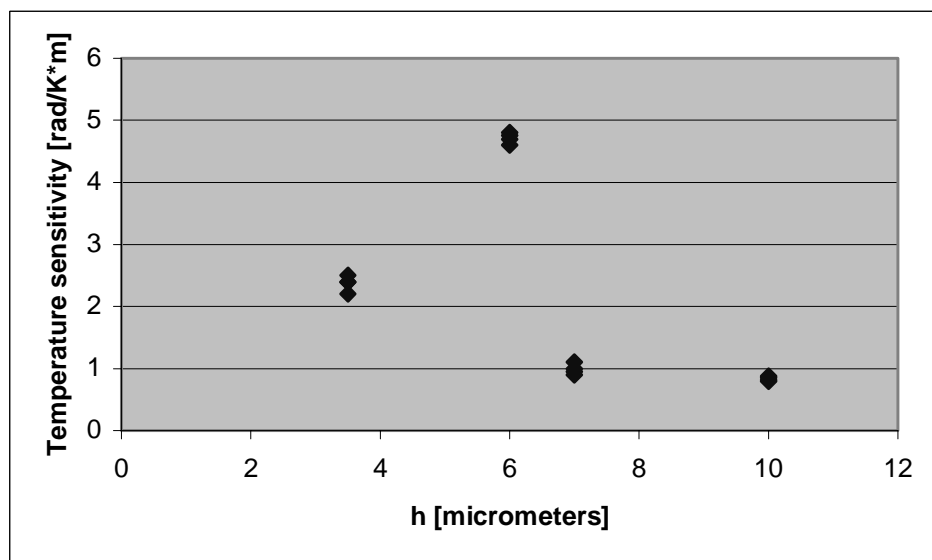
Fig. 5. The sensor properties measurements set

Fig. 6 presents results of the temperature sensitivity measurements for the dual core optical fibers with different distances between cores. The input polarization of light was parallel to the y direction (see fig. 1) and the examined direction of polarization of output light was parallel to the x direction.



*Fig. 6. Temperature sensitivity of the dual core optical fibers with different distances between cores. The polarization of input light was parallel to the y direction; examined direction of polarization of output light was parallel to the x direction*

Fig. 7 presents results of the temperature sensitivity when the input polarization of light was parallel to the x direction and the examined direction of polarization of output light was parallel to the y direction.



*Fig. 7. Temperature sensitivity of the dual core optical fibers with different distances between cores. The polarization of input light was parallel to the x direction; examined direction of polarization of output light was parallel to the y direction*

Tables 2–5 present results of measured sensitivities of dual core optical fibers.

Table 2

**Temperature sensitivity of the dual core optical fiber with  $h=3,5\mu\text{m}$   
for the different input and examined output light polarization**

Direction of polarization of input light	Examined direction of polarization of output light	Temperature sensitivity [rad/K*m]
parallel to y direction	parallel to x direction	3
parallel to x direction	parallel to y direction	2,2
at an angle of $45^0$ to x direction	at an angel of $45^0$ to x direction	8

Table 3

**Temperature sensitivity of the dual core optical fiber with  $h=6\mu\text{m}$   
for the different input and examined output light polarization**

Direction of polarization of input light	Examined direction of polarization of output light	Temperature sensitivity [rad/K*m]
parallel to y direction	parallel to x direction	4,6
parallel to x direction	parallel to y direction	4,6
at an angle of $45^0$ to x direction	at an angel of $45^0$ to x direction	12

Table 4

**Pressure sensitivity of the dual core optical fiber with  $h=7\mu\text{m}$   
for the different input and examined output light polarization**

Direction of polarization of input light	Examined direction of polarization of output light	Pressure sensitivity [rad/MPa*m]
parallel to y direction	parallel to x direction	0,45
parallel to x direction	parallel to y direction	0,45
at an angle of $45^0$ to x direction	parallel to y direction	0,9

Table 5

**Pressure sensitivity of the dual core optical fiber with  $h=3,5\mu\text{m}$   
for the different input and examined output light polarization**

Direction of polarization of input light	Examined direction of polarization of output light	Pressure sensitivity [rad/MPa*m]
parallel to y direction	parallel to x direction	1,5
parallel to x direction	parallel to y direction	1,5
at an angle of $45^0$ to x direction	parallel to y direction	4,2

#### 4. Summary and conclusions

The series of the dual core optical fibers with different distances between cores was manufactured with MCVD method.

The diameters of cores in all fibers were the same. The numerical aperture calculated from refractive index profile of prapreform I was small and it was equal to 0,142.

For characterization of the dual core optical fibers we applied measurements methods used to characterization of the low and high birefringent optical fibers.

It was defined dependences of the coupling length between cores as function of the temperature and pressure change for different distances between cores. In this paper they were defined as temperature and pressure sensitivity respectively.

The measured pressure sensitivity depends on input polarization of light and examined output polarization. It changes from 0,45rad/MPa\*m to 4,2rad/MPa\*m for two different fibers with change of input and output light polarization.

Measured temperature sensitivity depends on input polarization of light and examined output polarization too. It change from 3rad/K\*m to 12 rad/K\*m for two exemplary fibers. The change of  $K_T$  for different  $h$  indicates the existence of maximum. Its determination requires of further experimental investigations.

Probably the shape of dependence of  $K_T$  on  $h$  is caused by stress profile inside optical fiber in spite of small numerical aperture.

We hope that the planed experimental investigation of the analogous dependences in the dual core photonic crystal fibers may explain this problem.

1. Woliński T.R. *Polarimetric Optical Fibers and Sensors in Progress in Optics Vol.XL*, ed. E.Wolf (2000), 1-75.

2. Friberg S.R., Silberberg Y., Oliver M.K., Andrejco M.J., Saifi M.A., W.Smith P. *Ultrafast All-Optical Switching in a Dual-Core Fibre Nonlinear Coupler*, *Appl. Phys. Lett.* 51, (1987), 1135-1137.

3. Gang-Ding Peng, T.Tjugiarto, P.L.Chu. *Twin-core optical fiber with large core ellipticity*, *Appl. Opt.* Vol.30, No6, (1991), 632-634.

UDC 621.382

A.S.Andonova, N.G. Atanasova  
FETT, Technical University of Sofia,  
Sofia, Bulgaria

## TESTING ALGORITHMS FOR SCREENING OF LARGE ELECTRONIC SYSTEMS

© Andonova A.S., Atanasova N.G., 2004

**When a hardware system is screening, a problem is when to stop the test and accept the system. Based on this these, the paper describes and evaluates seven possible algorithms. Three of these algorithms as most promising are tested with simulated data. Different systems are simulated, and 50 Monte Carlo simulations made on each system. The stop times generated by the algorithm is compared with the known perfect stop time. Of the three algorithms two is selected as good. These two algorithms are then tested on real data. The algorithms are tested with three different levels of confidence. The number of correct and wrong stop decisions are counted. The conclusion is that the Weibull algorithm with 90% confidence level takes the right decision in every one of the cases.**

### 1. Introduction

When performing a run-in or acceptance testing on a large hardware system, it is often a problem to decide when to stop testing [1,2]. If it is stop too early the system will be delivered to the customer with too many early failures. On the other hand testing is very expensive, and the test can delay the delivery.

For hardware screening exist the same problem. A stress screening process will in the beginning precipitate many early failures per hour, but the last failures take a lot longer to precipitate. In the IEC standard IEC 61163-1 "Reliability stress screening of repairable items produced in lots" [3], the problem is solved by accepting that a sample of the product is run for an extended screening period, in order to find the optimum duration of the screening process. This duration is expressed as a failure free period. The aim is to stop the screening process as soon as the curve of the accumulated failures per 100 items levels out i.e. the curve converges towards a straight line as can be seen in fig. 1.